Coulomb Effects at Saddle-Type Critical Points

E. O. KANE
Bell Telephone Laboratories, Murray Hill, New Jersey 07974
(Received 1 August 1968; revised manuscript received 29 October 1968)

The effect of the Coulomb interaction between electron and hole at an M_1 (saddle-type) critical point is studied in the effective-mass approximation, using the adiabatic method first treated by Velický and Sak. The complete adiabatic potential for the heavy-mass degree of freedom is computed. The method is tested by calculating the binding energy for positive heavy mass and comparing it with Kohn and Luttinger's variational result. Reasonable accuracy for mass ratios greater than 5 is obtained. For negative heavy mass, the two-dimensional light-mass coordinates give a bound state which results in an effective repulsive potential. The contribution to ϵ_2, the imaginary part of the dielectric function, is computed, and a peak is found at the energy of the two-dimensional bound state. A sharp drop in ϵ_2 above the peak is found, which contrasts with the sharp drop below the peak for M_0 singularities. Quantitative agreement is found with the structure in ϵ_2 for CdTe at 3.5 eV measured by Marple and Ehrenreich, and it is expected that other L-point transitions in III-V semiconductors can be similarly interpreted.

I. SUMMARY

STRUCTURE in the fundamental optical reflectivity due to critical points has been widely used in the empirical determination of energy band structures by the pseudopotential method.[1] The importance of this application has motivated a considerable amount of effort to understand the form of the critical-point structure in greater detail.

If we expand the optical energy $\mathcal{E}_c(\mathbf{k})-\mathcal{E}_v(\mathbf{k})$ in a Taylor series about the critical point $\mathbf{k}_0$, we have

$$\mathcal{E}_c(\mathbf{k})-\mathcal{E}_v(\mathbf{k})=\hbar\omega_0+\hbar^2(k_i-k_{0i})^2/2m_i. \quad (1)$$

The linear terms are absent by definition. Critical points are of four types, designated M_j, where j refers to the number of reduced mass components m_i which are negative.

If one neglects correlation effects between the electron and hole, then all four types of critical points give a nonanalytic contribution to ϵ_2, the imaginary part of the dielectric constant, which is of square-root form.[1,2] The modification of this result due to the Coulomb attraction between electron and hole is very drastic for an M_0 singularity. Sharp exciton lines due to electron-hole bound states occur, and even the continuum absorption is strongly modified. These well-known results have been derived by Elliott[3] for the case of an isotropic positive mass.

For an M_3 singularity with isotropic negative mass, the Coulomb problem is also tractable and has been discussed by Velický and Sak.[4] The effect of the Coulomb interaction here is to suppress the critical-point structure. No bound states occur and the absorption near the edge is strongly suppressed, which will make M_3 singularities difficult to observe.

The situation at an M_1 singularity has been more controversial. Phillips[5] was the first to suggest that pronounced structure would result from Coulomb effects at M_1 singularities. He called the structure "saddle-point excitons." This view was challenged by Duke and Segall[6] who pointed out that for a monatomic attractive potential, resonant behavior in the negative-mass degree of freedom was impossible. They concluded that for some types of effective potential, structure in ϵ_2 at saddle points was still possible, but for the Coulomb potential treated in the adiabatic approximation they did not find important structure.

Several authors have stressed the importance of central cell corrections when electron-hole correlations are strong. This approach goes beyond the effective-mass approximation and hence depends strongly on what is assumed about the over-all band structure. Velický and Sak,[4] using a δ-function interaction, found that the optical critical points remained fixed in energy but were strongly modified in shape by the interaction, M_1 singularities being enhanced and M_2 suppressed. Toyozawa *et al.*,[7] who also used a short-range interaction, found modification of band critical points and additional new resonance-type structure associated with bound states of the short-range interaction. Hermanson[8] used a longer-range interaction and also found resonances of the Toyozawa type. The association of these resonances with critical points was not completely unambiguous but tended to support Phillips's interpretation.

Velický and Sak[4] also treated the case of an M_1 singularity without central cell effects but they used Coulomb interaction. They treated the problem by the adiabatic (Born-Oppenheimer) approximation which is valid when the negative mass is much larger in absolute value than the positive masses. They found structure associated with the lowest bound state of the two-dimensional hydrogenic spectrum of the positive-mass

[1] J. C. Phillips, in *Solid State Physics*, edited by F. Seitz and D. Turnbull (Academic Press Inc., New York, 1966), Vol. 18, p. 55.
[2] D. Brust, Phys. Rev. **134**, A1337 (1964).
[3] R. J. Elliott, Phys. Rev. **108**, 1384 (1957).
[4] B. Velický and J. Sak, Phys. Status Solidi **16**, 147 (1966).
[5] J. C. Phillips, Phys. Rev. **136**, A1705 (1964).
[6] C. B. Duke and B. Segall, Phys. Rev. Letters **17**, 19 (1966).
[7] Y. Toyozawa, M. Inoue, T. Inui, M. Ozaki, and E. Hanamura, J. Phys. Soc. Japan **21**, 133 (1966); Suppl. **21**, 133 (1966).
[8] J. Hermanson, Phys. Rev. **166**, 893 (1968).

degrees of freedom. Their results were rather incomplete, however.

We have extended the calculations of Velický and Sak[4] and have numerically computed the effective adiabatic potential as a function of the heavy-mass coordinate. This effective potential can, of course, be used for either sign of heavy mass. For the positive heavy-mass case, we have tested the adiabatic approximation by computing the lowest bound state and comparing it with the binding energy calculated by a variational form due to Kohn and Luttinger.[9] The adiabatic results were reasonable down to mass ratios of the order of 5, but were not an improvement on Kohn-Luttinger unless the mass ratio was greater than 80.

For the negative heavy-mass case (M_1), we have calculated the saddle-point line shape and find definite structure associated with the lowest two-dimensional bound state of the light-mass degrees of freedom, as expected from Velický and Sak's work. The peak is asymmetrical and drops much more sharply on the high-energy side, just the opposite of the lifetime-broadened M_0 line shape. This fact should permit a clear distinction between the two types of critical points, provided central cell corrections are not dominant. Band-structure effects beyond the effective-mass approximation may also distort the line shape considerably. The adiabatic approximation is likely to be good for M_1 (or M_0) critical points occurring on symmetry lines. The transverse masses will be equal by symmetry, and are likely to be much smaller than the longitudinal mass, since $\Delta\mathbf{k}\cdot\mathbf{p}$ breaks the symmetry when $\Delta\mathbf{k}$ is transverse to the symmetry axis. The broken symmetry allows interaction between bands of different symmetry, which are usually closer together than bands of the same symmetry.

The interpretation of the structure that we observe in our calculation is identical to that given by Duke and Segall[6] for structure they obtained using a parabolic separable potential. However, by virtue of our more detailed calculations, we conclude that Coulomb effects do lead to pronounced structure at saddle-point edges.

A strong asymmetric line shape was observed in CdTe at 3.5 eV by Marple and Ehrenreich.[10] They interpreted this shape on a pure density-of-states basis, invoking a rather special band structure. Phillips[1] suggested that a more likely explanation could be based on "saddle-point excitons." In Sec. III, we discuss the case of CdTe in detail and show that we can get quantitative agreement between our calculations and Marple and Ehrenreich's data[10] using only one adjustable parameter, the longitudinal reduced mass, which has not been determined from other measurements. On the basis of this detailed agreement, it seems likely that most if not all of the "L point" line shapes in column-IV, III-V, and II-VI semiconductors can be explained in a similar manner. Shaklee, Rowe, and Cardona[11] have argued that the line shape of InSb near 1.9 eV suggests that Coulomb effects play a dominant role. Since the line shape of InSb is very similar to CdTe, our results support this conclusion.

[9] W. Kohn and J. M. Luttinger, Phys. Rev. **98**, 915 (1955).
[10] D. T. F. Marple and H. Ehrenreich, Phys. Rev. Letters **8**, 87 (1962).

II. ADIABATIC APPROXIMATION

Our calculation follows very closely the assumptions and approximations made by Velický and Sak.[4] We wish to calculate the contribution to $\epsilon_2(\omega)$ from the vicinity of an M_1 critical point. ϵ_2 is given by[2]

$$\epsilon_2(\omega)=\frac{4\pi^2e^2}{3m^2\omega^2\mathcal{V}}\sum_f|\mathbf{p}_{if}|^2\delta(E_f-E_i-\hbar\omega), \qquad (2)$$

where $\mathbf{p}_{if}$ is the matrix element of momentum between initial and final states, and $\mathcal{V}$ is the volume. There is a δ function for energy conservation and a sum over final states f. m is the free electron mass.

If we make the effective-mass approximation for the exciton, Elliott[3] has shown that the matrix element p_{if} can be written

$$p_{if}=\langle u_i|\,p\,|u_f\rangle\Phi(0)\sqrt{\mathcal{V}}, \qquad (3)$$

where $\Phi(r)$ is the exciton envelope function and u_i and u_f are the cell-periodic parts of the Bloch function at the critical point. The Schrödinger equation for the envelope function is

$$(p_1^2/2m_1+p_2^2/2m_2+p_3^2/2m_3-e^2/\kappa r)\Phi=E\Phi. \qquad (4)$$

We will then have

$$\hbar\omega=E+E_c, \qquad (5)$$

where E_c is the one-electron band energy at the critical point. We use E_c as our energy zero throughout this paper.

We solve Eq. (4) in the adiabatic approximation by assuming $m_1=m_2>0$, $|m_3|\gg m_1$. The adiabatic method assumes the variational form[12]

$$\Phi_{nm}(\boldsymbol{\varrho},z)=\varphi_n(\boldsymbol{\varrho},z)\psi_{nm}(z), \qquad (6)$$

with φ_n defined by

$$\{p_1^2/2m_1+p_2^2/2m_2-e^2/\kappa(\rho^2+z^2)^{1/2}\}\varphi_n(\boldsymbol{\varrho},z)=V_n(z)\varphi_n(\boldsymbol{\varrho},z). \qquad (7)$$

$\boldsymbol{\varrho}$ refers to the light-mass degrees of freedom, 1 and 2, and z refers to the heavy-mass coordinate 3. z is a fixed parameter in Eq. (7) in accord with the idea that it varies slowly compared to $\boldsymbol{\varrho}$. $V_n(z)$ is the eigenvalue for Eq. (7). Using a variational method, $\psi_{nm}(z)$ is found to

[11] K. L. Shaklee, J. E. Rowe, and M. Cardona, Phys. Rev. **174**, 828 (1968).
[12] A. Messiah, *Quantum Mechanics* (North-Holland Publishing Co., Amsterdam, 1962), Vol. II, p. 789.

be determined by the eigenvalue equation[12]

$$\{p_3^2/2m_3+V_n(z)+W_n(z)\}\psi_{nm}(z)=E_{nm}\psi_{nm}(z), \quad (8)$$

$$W_n(z)=\frac{1}{2m_3}\int\left|\frac{\partial\varphi_n(\varrho,z)}{\partial z}\right|^2 d\varrho. \quad (9)$$

$W_n(z)$ is clearly the extra kinetic energy coming from the parametric dependence of φ on z. This term is frequently left out of adiabatic calculations and we find that it is indeed small though not negligible. It is important to include it because otherwise the results are not variational and one cannot guarantee that the lowest eigenvalues of Eq. (8) are upper bounds for the true eigenvalues of Eq. (4).

We work throughout in atomic units of the light-mass problem, i.e., we set $m_1=e^2/\kappa=\hbar=1$. The unit of length is then

$$a_1=\hbar^2\kappa/m_1e^2 \quad (10)$$

and the unit of energy (double "rydbergs")

$$E_{B1}=m_1e^4/(\hbar^2\kappa^2). \quad (11)$$

We can derive analytic expressions for $V_n(z)$, $W_n(z)$, and $\varphi_n(z)$ for $|z|\gg1$ and $|z|\ll1$. Some of these results were given by Velický and Sak.[4] The two-dimensional Coulomb problem is treated extensively by Flügge and Marschall[13]:

$$V_n(z)=-1/2(n+\tfrac{1}{2})^2+2\pi|\varphi_n(0)|^2|z|; \quad |z|\ll1 \quad (12)$$

$$|\varphi_n(0)|^2=1/\pi(n+\tfrac{1}{2})^3; \quad n=0,\ 1,\ 2,\cdots \quad (13)$$

$$|\varphi_{k1}(0)|^2\frac{dn}{dE_1}=\frac{1}{\pi}\frac{1}{1+e^{-2\pi/k_1}}, \quad (14)$$

$$\tfrac{1}{2}k_1^2=E_1, \quad (15)$$

$$W_0(z=0)=\frac{1}{2m_3}\sum_j\left\{\frac{2\pi\varphi_j(0)\varphi_0(0)}{E_0-E_j}\right\}^2 \simeq 9.289/m_3, \quad (16)$$

$$V_0(z)=-1/|z|+1/|z|^{3/2}; \quad |z|\gg1 \quad (17)$$

$$W_0(z)=9/32z^2; \quad |z|\gg1. \quad (18)$$

$V_n(0)$ and $\varphi_n(0)$ are obtained from the solutions of the two-dimensional Coulomb problem. Equations (12) and (16) are obtained by first-order perturbation theory. It is clear from Eq. (7) that the region $\rho>z$ only gives contributions to terms of order z^2 or higher. Hence the nonanalytic terms in $|z|$ can all be expressed in terms of $\varphi_n(0)$.

In Eq. (14), dn/dE_1 is the two-dimensional density of states of the light-mass coordinates.

[13] S. Flügge and H. Marschall, *Rechenmethoden der Quantentheorie* (Julius Springer-Verlag, Berlin, 1952), p. 80.

Equations (17) and (18) are obtained by expanding $(\rho^2+z^2)^{-1/2}$ to terms of order ρ^2 which gives harmonic-oscillator wave functions.

Using Eq. (13), it is easily seen that the term $n=0$ contains 95% of the oscillator strength associated with the two-dimensional discrete spectrum. Hence we consider only $n=0$ in what follows. We will consider the contribution from the two-dimensional continuum, however, as given by Eq. (14). The adiabatic potential $V_k(z)=E_1$, where E_1 is the light-mass kinetic energy, independent of z. This is because nondiagonal terms in k are neglected and the diagonal term makes a negligible contribution to E_1.

The adiabatic approximation is presumably less accurate for continuum problems because the states of the unperturbed problem whose mixing is neglected lie so close together in this case. For lack of a better simple alternative we make the approximation anyway. The term $W_k(z)$ in Eq. (9) is also zero in the limit of infinite volume. Hence we take the $\psi_{km}(z)$ functions as plane waves.

The quantities $V_n(z)$ and $W_n(z)$ in Eqs. (7)–(9) have been computed numerically for the ground state $n=0$ by straightforward integration of Eq. (7) with the eigenvalue $V_0(z)$ determined to prevent $\varphi_0(\rho,z)$ from blowing up as $\rho\to\infty$. $d\varphi_0/dz$ was determined by differentiating Eq. (7) with respect to z and integrating the resulting inhomogeneous equation. The proper amount of the homogeneous solution was determined by differentiating the normalization integral

$$\frac{d}{dz}\int\varphi_0^2(z,\varrho)d\varrho=2\int\varphi_0(z,\varrho)\frac{d\varphi_0}{dz}(z,\varrho)d\varrho =0. \quad (19)$$

The quantity dV_0/dz which arises in the differentiation of Eq. (7) was computed by the first-order perturbation result

$$\frac{dV_0}{dz}=-\int\varphi_0^2(z,\varrho)\frac{d}{dz}\frac{e^2}{\kappa(\varrho^2+z^2)^{1/2}}d\varrho. \quad (20)$$

The results of the calculation are given in Table I and plotted in Figs. 1 and 2. It is clear from Fig. 1 that Eq. (12) is a very poor approximation to $V_0(z)$ except for very small values of z.

The calculated values suggest that $W_0(z)$ approaches $W_0(0)$ like $W_0(0)+a\sqrt{z}$, but we have not verified this analytically.

The adiabatic approximation can be used for either sign of heavy mass m_3, as long as $|m_3|\gg m_1=m_2$. A convenient test of the adiabatic results can be obtained by computing the lowest bound state in the adiabatic potential for m_3 positive and comparing it with the values computed from the variational form

$$\Phi(\mathbf{r})=(1/N)e^{-(a\rho^2+bz^2)^{1/2}}, \quad (21)$$

TABLE I. Contributions to the adiabatic potential versus z, the heavy-mass coordinate in a.u. The $V_0(z)$ is the Coulomb contribution; $m_3W_0(z)$ is the extra kinetic-energy contribution. On the basis of varying the interval of integration, the last digit quoted is believed to have some significance. $V_0(z)$ and $W_0(z)$ are defined in Eqs. (7) and (8).

$V_0(z)$	$m_3W_0(z)$	z
−2.00	9.289	0
−1.99	8.5	0.000978
−1.97	8.1	0.00196
−1.94	7.3	0.00391
−1.92	6.8	0.00587
−1.87	5.9	0.00978
−1.82	5.2	0.0137
−1.75	4.31	0.0215
−1.68	3.65	0.0294
−1.56	2.79	0.0450
−1.47	2.24	0.0607
−1.32	1.58	0.0920
−1.21	1.19	0.123
−1.04	0.78	0.186
−0.925	0.56	0.248
−0.763	0.35	0.374
−0.656	0.23	0.499
−0.519	0.14	0.749
−0.434	0.09	1.00
−0.359	0.06	1.33
−0.271	0.03	1.98
−0.220	0.02	2.63
−0.162		3.91
−0.130		5.15
−0.0937		7.58
−0.0749		9.90
−0.0539		14.3
−0.0435		18.3
−0.0318		25.6
−0.0262		32.0
−0.0200		42.6
−0.0171		51.0
−0.0139		63.6
−0.0123		72.5
−0.0107		84.3
−0.0098		91.8
−0.0090		101

first used by Kohn and Kuttinger.[9] Equation (21) is exact for $m_3=m_1$; hence, it should serve as a good test of the adiabatic results in the region where they are worst.

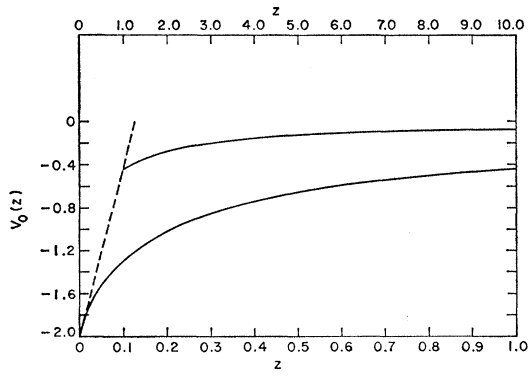

FIG. 1. Coulomb part of adiabatic potential $V_0(z)$ as a function of heavy-mass coordinate z. Light-mass atomic units. Upper abscissa goes with upper graph. Dashed line is small z asymptote. $V_0(z)$ is defined in Eq. (7). The light-mass atomic units are defined in Eqs. (10) and (11).

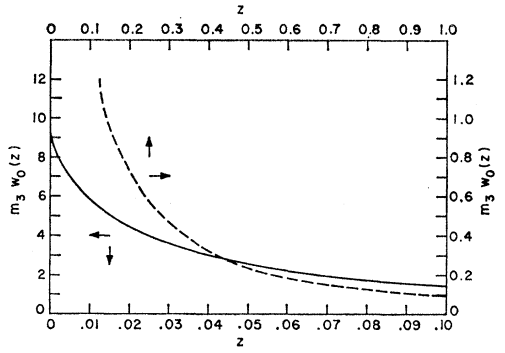

FIG. 2. Extra kinetic-energy part of adiabatic potential $m_3W_0(z)$ versus z. Upper-right scales go with dashed curve, lower left with solid curve. $W_0(z)$ is defined in Eq. (8). The light-mass atomic units are defined in Eqs. (10) and (11).

In Fig. 3 the dashed line is the binding energy from the variational form of Eq. (21) as a function of mass ratio, m_3/m_1. The solid line is the binding energy computed using the adiabatic potential, $V_0(z)+W_0(z)$, of Figs. 1 and 2. For a mass ratio of 5, the adiabatic energy is about 20% in error. The adiabatic result is not an improvement over the Kohn-Luttinger result until the mass ratio is greater than 80. The contribution of the $W_0(z)$ term to the binding energy was $\sim+30\%$ at a mass ratio of 6, $+9\%$ at 20, and $+1\%$ at 200. If we

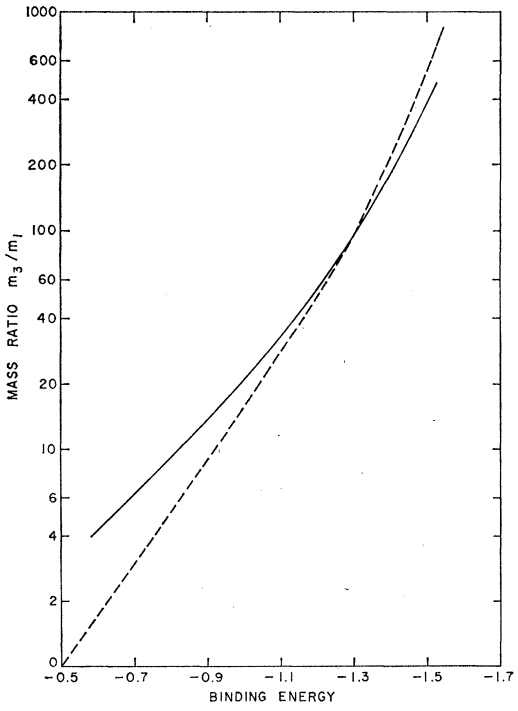

FIG. 3. Hydrogenic ground-state binding energy as a function of ellipsoidal mass ratio m_3/m_1. Light-mass atomic units. Dashed curve is energy computed by Kohn-Luttinger variational function. Solid line is computed using the adiabatic approximation. The light-mass atomic units are defined in Eqs. (10) and (11).

had ignored this term, the adiabatic results would have appeared to be better than they really are.

We conclude from this comparison that the adiabatic method is reasonably reliable down to mass ratios of the order of 5.

For the negative-mass case, we have used the adiabatic potential in Eq. (8) to compute $|\psi_{nm}(0)|^2$. This was done by integrating the equation from the origin to a sufficiently large value of z, so that the WKB approximation could be adopted,

$$\psi(z)=\frac{a}{|E_{0k}-V_0(z)-W_0(z)|^{1/4}} \times\exp\left\{i\int_0^z k(z')dz'+ib\right\}, \quad (22)$$

$$k^2(z)/2m_3+V_0(z)+W_0(z)=E_{0k}. \quad (23)$$

The integration determined a and b, and the wave function was then scaled to give unit normalization. Since the potential $V(z)$ is symmetric, the wave functions are even $[\psi'(0)=0]$ or odd $\psi(0)=0$. Only even states contribute to ϵ_2 by Eq. (3). The one-dimensional density of even states per unit length without spin is

$$\frac{dn}{dE_3}=\frac{1}{4\pi}\left|\frac{m_3}{2E_3}\right|^{1/2}. \quad (24)$$

The quantity

$$S_0(E_3)\equiv|\varphi_0(0)|^2|\psi_{0E}(0)|^2 dn/dE_3 \quad (25)$$

is plotted in Fig. 4 for mass ratios $m_3=-5$, -40, and -320.

The shape of the curve is easily interpreted. For an energy E_{0k} well below the minimum of the adiabatic potential, the WKB approximation is applicable, and the value of $|\psi(0)|^2$ is proportional to

$$[E_{0k}-V_0(0)-W_0(0)]^{-1},$$

which increases as E_{0k} increases. When E_{0k} is greater than the bottom of the barrier, the particle must "tunnel" to the origin (because of the negative mass) and the value of $|\psi(0)|^2$ drops rapidly. The peak occurs near -2, the value of the light-mass binding energy. The curve broadens as the mass ratio decreases (in absolute value), but the dependence on mass is rather weak. The high-energy dropoff due to tunneling remains abrupt. Figure 1 suggests that the tunneling penetration of the true $V_0(z)$ is very much less than it would be for the triangular potential which it approaches asymptotically at small z.

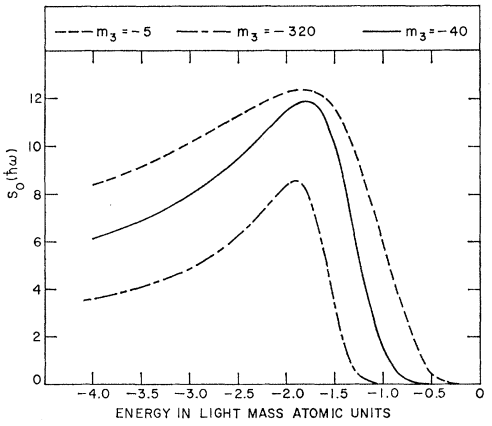

FIG. 4. $S_0(\hbar\omega)$ versus $\hbar\omega$ in light-mass atomic units. Contribution to the dielectric function from the two-dimensional ground state for three negative masses (M_1 singularity). Energy zero at the critical point. S_0 is plotted for $m_3=-320$, $5S_0$ for $m_3=-40$, and $20S_0$ for $m_3=-5$.

The total oscillator strength of the higher two-dimensional bound states is only 5% of that of the ground state, so we neglect them. We must include the two-dimensional continuum, however. The adiabatic approximation is less reliable and we cannot trust the continuum structure that we find, but we wish to know if the continuum contribution will "wash out" the bound-state structure. The results say that it does not, and we feel that the approximation is adequate to justify this conclusion.

In the adiabatic approximation for φ_k in the continuum, ψ_{km} is a plane wave, so that we can write

$$|\psi_{E3}(0)|^2\frac{dn}{dE_3}=\frac{1}{2\pi}\left|\frac{m_3}{2E_3}\right|^{1/2} \quad (26)$$

(spin is not included). We must multiply Eq. (26) by Eq. (14) and integrate $dE_1dE_3\delta(E_1+E_3-\hbar\omega)$ with the δ function for energy conservation. This gives the continuum analog of Eq. (25),

$$S_{\rm cont}{}^1(\hbar\omega)\equiv\int\int|\varphi_{E1}(0)|^2|\psi_{E3}(0)|^2\frac{dn}{dE_1}\frac{dn}{dE_3} \times\delta(E_1+E_3-\hbar\omega)dE_1dE_3. \quad (27)$$

The total contribution to $\epsilon_2(\hbar\omega)$ is then

$$\epsilon_2(\hbar\omega)=c\omega^{-2}[S_0(\hbar\omega)+S_{\rm cont}{}^1(\hbar\omega)], \quad (28)$$

where c is independent of ω.

Substituting Eqs. (14) and (26) into Eq. (27), we have

$$S_{\rm cont}{}^1(\hbar\omega)=\alpha\int_{\hbar\omega}^{E_K}f(\hbar\omega,E_1)dE_1; \quad \hbar\omega>0$$

$$=\alpha\int_0^{E_K}f(\hbar\omega,E_1)dE_1; \quad \hbar\omega<0 \quad (29)$$

$$\alpha=\sqrt{m_3}/2\pi^2\sqrt{2}, \quad (30)$$

$$f(\hbar\omega,E_1)=[(E_1-\hbar\omega)^{1/2}]^{-1} \times(1+\exp[-2\pi/(2E_1)^{1/2}])^{-1}. \quad (31)$$

The limits of integration are determined by the requirements $E_1>0$, $E_3<0$. An energy cutoff $E_1\leq E_\kappa$ has been introduced to make the integrals finite. Although the value of $S_{\rm cont}{}^1(\hbar\omega)$ depends on the choice of E_κ, the $\hbar\omega$ dependence of $S_{\rm cont}{}^1$ will not depend on E_κ provided $E_\kappa\gg\hbar\omega$. Hence, we are led to define the quantity

$$S_{\rm cont}(\hbar\omega)\equiv\lim_{E_\kappa\to\infty}\left\{S_c{}^1(\hbar\omega)-\alpha\int_0^{E_\kappa}f(0,E_1)dE_1\right\}. \quad (32)$$

We have subtracted off a quantity, independent of ω, which tends to ∞ as $E_\kappa\to\infty$, so that the resulting S_c is finite. This is permissible, since we are only interested in structure near the critical energy $\hbar\omega_c$. We must assume that $\mathbf{k}$ points far from the critical point $\mathbf{k}_c$ do not contribute to this structure. Such contributions could not be treated in the effective-mass approximation in any case.

The following limiting expressions for the function $S_{\rm cont}(\hbar\omega)$ are easily established:

$$\begin{aligned}S_{\rm cont}(\hbar\omega)&\simeq-2\sqrt{2}\alpha(\hbar\omega)^{1/2}/\pi; \quad \omega<0,\ |\omega|\ll1\\ &\simeq-\sqrt{2}\alpha(\hbar\omega)^{1/2}/\pi; \quad \omega<0,\ |\omega|\gg1\\ &\simeq-(\ln2)\alpha\hbar\omega/\pi^2; \quad \omega>0,\ |\omega|\ll1\\ &\simeq-\tfrac{1}{2}\alpha\ln(2\hbar\omega/\pi^2); \quad \omega>0,\ |\omega|\gg1. \quad (33)\end{aligned}$$

The complete function $S_{\rm cont}(\hbar\omega)$ is readily computed numerically. We have plotted the combined function

$$S_{\rm tot}(\hbar\omega)=S_0(\hbar\omega)+S_{\rm cont}(\hbar\omega) \quad (34)$$

in Fig. 5 for three values of the mass ratio, $m_3=-5$, -40, and -320. The continuum structure occurs at the critical point E_c (our energy zero) as expected, but is relatively weak compared to the structure associated with the two-dimensional bound state.

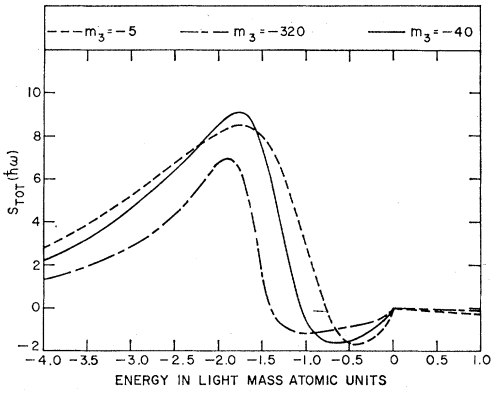

FIG. 5. $S_{\rm tot}(\hbar\omega)$ versus $\hbar\omega$ in light-mass atomic units. Total contribution to the dielectric function from the continuum and discrete states of the light-mass spectrum for three negative masses (M_1 singularity). Energy zero at the critical point. $S_{\rm tot}$ is plotted for $m_3=-320$, $5S_{\rm tot}$ for $m_3=-40$, and $20S_{\rm tot}$ for $m_3=-5$.

The most characteristic feature of the M_1 saddle point with Coulomb effects appears to be the steep dropoff on the high-energy side associated with the tunneling penetration of the barrier in the adiabatic approximation. Where the adiabatic approximation does not apply, much less pronounced structure is anticipated. Of course, we have neglected central cell corrections and contributions from $\mathbf{k}$-space regions far from the critical point, which may lead to structure in special cases.

In conclusion, we have shown that M_0 and M_1 singularities with strong Coulomb effects can be distinguished by noting the steep slopes on the low- and high-energy sides of the singularities, respectively.

III. APPLICATION TO CdTe

The close resemblance between our results and the line shape of CdTe as measured by Marple and Ehrenreich[10] was brought to our attention by Phillips. We can make reasonable estimates of the parameters of our model appropriate to this case and show that their data appears to be quite well described by our theory.

We begin by estimating the momentum matrix element

$$P\equiv\langle\Gamma_1|p_x|\Gamma_{15x}\rangle \quad (35)$$

at $k=0$ using Kanazawa and Brown's[14] measurement of the conduction-band mass, $m_c=0.096m_0$. We assume a three-band formula

$$\frac{1}{m_c{}^*}=\frac{1}{m_0}+\frac{2\hbar^2}{m_0{}^2}\left(\frac{2}{3}\frac{P^2}{E_{G0}}+\frac{1}{3}\frac{P^2}{E_{G0}+\Delta_0}\right). \quad (36)$$

We use $E_{G0}=1.61$ eV[15] and $\Delta_0=0.81$ eV.[16] This gives $P^2=0.31$ a.u. which is to be compared with $P^2=0.47$ a.u. for Ge, also at $k=0$.

We can then use this result to estimate the mass at L. The equivalent three-band formulas are

$$\begin{aligned}\frac{1}{m_{c\perp}{}^*}&=\frac{1}{m_0}+\frac{2\hbar^2}{m_0}\left(\frac{1}{2}\frac{P^2}{E_{G1}}+\frac{1}{2}\frac{P^2}{E_{G1}+\Delta_1}\right),\\ \frac{1}{m_{v\perp}{}^*}&=\frac{1}{m_0}+\frac{2\hbar^2}{m_0}\frac{1}{2}\left(\frac{P^2}{-E_{G1}}\right).\end{aligned} \quad (37)$$

We use $E_{G1}=3.60$ eV, $\Delta_1=0.55$ eV from Marple's data.[10] The reduced mass $m_{r\perp}{}^{*-1}=m_{c\perp}{}^{*-1}-m_{v\perp}{}^{*-1}$ is equal to $6.8\,m_0{}^{-1}$. The analogous procedure applied to Ge yields the transverse conduction-band mass accurate to 2%. Stated differently, the value of P^2 at the L point in Ge is 0.48 a.u., only 2% higher than the value at Γ. This result gives us confidence in our procedure. However, it should be noted that the three-band formulas are not expected to be as accurate for CdTe as for Ge,

[14] K. K. Kanazawa and F. C. Brown, Phys. Rev. **135**, A1757 (1964).
[15] D. T. F. Marple, Phys. Rev. **150**, 728 (1966).
[16] M. Cardona and D. L. Greenaway, Phys. Rev. **131**, 98 (1963).

both because the band gaps are larger in comparison to the energies of bands which are neglected and because the symmetry is lower, which means that more bands "interact" in the zinc blende than in the diamond lattice.

To calculate the "light-mass atomic unit" of energy in Eq. (11), we need a "dielectric constant." We use $\kappa_\infty = 7.05$.[17] The light-mass atomic unit then is 0.080 eV. Since the light-mass binding energy is then 0.16 eV, the use of κ_∞ rather than κ_0 is justified since the phonon energy is of the order of 0.02 eV.

Equation (2) for ϵ_2 can be written in terms of $S_{\rm tot}$ of Eq. (34),

$$\epsilon_2(\omega) = \frac{8\pi^2(m_{r1}^*/m_0)^2\langle p^2\rangle_{\rm av} N S_{\rm tot}(\hbar\omega)}{3m_0^2 a_0^2 \kappa_\infty}. \quad (38)$$

Here a_0 is the real Bohr radius, N is the number of critical points, and $\langle p^2\rangle_{\rm av}$ is the average value of $|p_x|^2$, say, averaged over the N extrema. Equation (38) refers to the contribution from one of the spin-orbit split pair of bands (counting its Kramers degeneracy, of course). The average value of $|p_x|^2$ is $\frac{1}{3}P^2$ and we take $N=4$, assuming the transition is at L. Substituting in Eq. (38), we have

$$\epsilon_2(\omega) = 2.1 S_{\rm tot}(\hbar\omega) \quad (39)$$

for CdTe near 3.5 eV.

In Fig. 6, we have used Marple's data[10] (see Acknowledgments) to separate out the contribution from one of the spin-orbit split bands by assuming that both bands give contributions of the same shape and amplitude but shifted by 0.55 eV relative to each other. In Fig. 5, we have arbitrarily taken our energy zero and our zero of $S_{\rm tot}$ to coincide. With this same zero, the experimental amplitude at the 3.46-eV peak is 5.0, which requires $S_{\rm tot}(\text{peak}) = 2.4$. Considering the amplitudes in Fig. 5, we estimate that this would correspond to a longitudinal-to-transverse mass ratio of about -60. We have accordingly used the computed line shape for mass ratio -40 and scaled the amplitude to make the peaks agree. The energy scale is fixed by the "light-mass atomic unit" which was calculated to be 0.080 eV. It is seen that the energy scale agrees extremely well. The amplitude, of course, was fitted by choosing a mass ratio of -60. We don't know of any other determination of this quantity. If it really is this large, it would be difficult to compute theoretically even from a very good pseudopotential band structure. We do not consider this to be a reliable determination of the mass ratio. A variation of a factor of 2 in the determination of ϵ_2 would lead to about a factor 2 change in mass ratio.

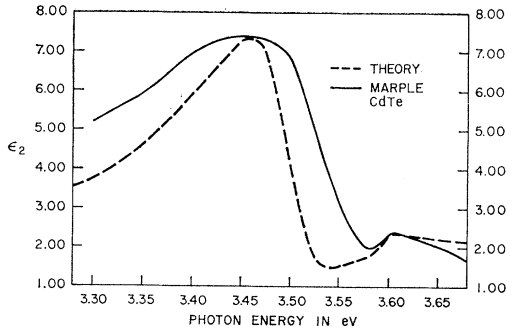

FIG. 6. The solid curve is the contribution of one of the spin-orbit components to $\epsilon_2(\omega)$ in CdTe, extracted from Marple and Ehrenreich's data (Ref. 10). The theoretical curve, shown dashed, is computed from the theory of the present paper using parameters discussed in the text. The vertical scale was "adjusted" by use of a mass ratio of -60. Introduction of lifetime broadening into the theoretical curve would clearly improve the agreement.

The theoretical curve shape is seen to agree fairly well with the experimental shape except that the experimental shape is significantly broader. Lifetime broadening is the most likely source of the discrepancy. In this case, the experimental and theoretical curves should have been matched in area rather than peak amplitude, which would require a somewhat larger mass ratio. Nonparabolic effects along the Λ line would be expected to increase the theoretical curve somewhat on the low-energy side.

In summary, the agreement between theory and experiment in Fig. 6 constitutes strong support for the present interpretation of this structure as due to Coulomb effects at a saddle point in the effective-mass approximation. Central cell effects and nonparabolic effects do not appear to be of major importance in determining the characteristic shape of the structure.

It appears likely that the shape of most of the other "L-type" critical points which are generally similar to CdTe can also be explained in this way. InSb seems to be a particularly clear cut example. The importance of Coulomb effects in the interpretation of the InSb spectrum has recently been stressed by Shaklee, Rowe, and Cardona.[11] The importance of exciton effects in CdTe were first suggested by Cardona and Harbeke[18] and later reemphasized by Cardona.[19] Phillips has suggested the importance of Coulomb effects at saddle points in a wide variety of materials,[1] including alkali halides. The present calculation seems to apply fairly well to columns IV, III–V, and II–VI semiconductors. It is not clear at present whether it can be applied to the alkali halides, since "central cell" corrections are presumably much more important in these materials.

Note added in proof. The author would like to note that the importance of exciton effects at Λ critical points was also suggested by Y. Hamakawa, F. Germano, and P. Handler, J. Phys. Soc. Japan Suppl. **21**, 111 (1966).

ACKNOWLEDGMENTS

The author is very grateful to D. T. F. Marple for access to his original data on CdTe. He also wishes to thank J. C. Phillips for useful suggestions and E. I. Blount for helpful discussions.

[17] B. Segall, Phys. Rev. **150**, 734 (1966).

[18] M. Cardona and G. Harbeke, Phys. Rev. Letters **8**, 90 (1962)

[19] M. Cardona, J. Appl. Phys. **36**, 2181 (1965).